Archaeometry 37, 2 (1995), 257–270. Printed in Great Britain

A PILOT STUDY IN NON-CONTACT LASER PHOTOTHERMAL ARCHAEOMETRY OF ANCIENT STATUARY PEDESTAL STONES FROM CYPRUS*

A. MANDELIS, K. McALLISTER,

Photothermal and Optoelectronic Diagnostics Laboratory, Department of Mechanical Engineering, University of Toronto, Toronto, M5S 1A4, Canada

C. CHRISTOFIDES

Department of Natural Sciences, Faculty of Pure and Applied Sciences, University of Cyprus, P.O. Box 537, Nicosia, Cyprus

and C. XENOPHONTOS

Geological Survey Department, Nicosia, Cyprus

Several samples of geological stones from statuary pedestals found in various archaeological sites in Cyprus have been characterized using non-contact laser infrared photothermal radiometry. Thermal diffusivities and effective optical absorption coefficients were calculated using a one-dimensional thermal-wave model. The mean values and standard deviations were tabulated and comparisons were made with lithographic and petrographic studies of the samples. Good correlations were found, thus demonstrating that laser photothermal archaeometry is a promising methodology for the accurate, potentially non-destructive and convenient characterization of the origins of ancient stones in Cyprus and other geological and archaeological sites.

KEYWORDS: CYPRUS, THERMAL WAVES, LASER PHOTOTHERMAL ARCHAEOMETRY, THERMAL DIFFUSIVITY, NON-CONTACT ANALYSIS, MARBLE, STATUARY PEDESTALS, LIMESTONE, CALCARENITE, CHARACTERIZATION, SOURCE

INTRODUCTION

The use of thermal diffusivity as a characterization quantity of rocks has been fairly widespread in recent decades (Somerton 1992). This property has attracted much attention owing to the fact that it is readily available from the analysis of transient thermal experiments upon solution of the equation for heat conduction in a given geometry. Although thermal diffusivity is easily accessible, in principle, as the thermophysical property responsible for thermal energy transport in matter, no experimental techniques have been developed for the study of rocks which combine accuracy of measurement and convenient, non-contact methodology. Both these features are essential if accurate determinations of the origins of ancient artefacts, such as statuary, are to be made through correlations based on the values of thermophysical properties of the artefacts. In most reported techniques, sample preparation and thermal detector/probe attachments may

* Received 14 March 1994, accepted 30 September 1994.

easily cause severe perturbations to the state or integrity of the sample, resulting in non-representative values of the thermal diffusivity. The intrusive nature of existing instrumentation and measurement methodologies of rocks creates the possibility of introducing large data scatter, which makes it difficult to apply to archaeometric investigations of the origins of ancient stones: in many such cases small compositional variations are expected between, say, marbles produced in neighbouring locations in the ancient world. Reliable characterization of such specimens requires improved technique resolution with minimal or no intrusion of the measurement methodology.

The most popular techniques to-date for the measurement of rock thermophysical properties include the Boozer method (Boozer 1958) and other transient methods by Mossahebi (1966), Gomaa (1973), Hirsh (1973) and Nguyen (1974). Boozer's method entails heating a cylindrical rock test specimen at a constant heating rate at the outside circumference and recording the temperature difference between the outer radius and the centre of the test specimen. Details of the experimental apparatus were given by Somerton and Boozer (1960 and 1961). The transient techniques utilized by other investigators (Mossahebi 1966; Gomaa 1973; Hirsch 1973; Nguyen 1974) also require intrusive contact of the heating elements(s) to the sample. For example, Nguyen (1974) used a paste-on heater. Hanley *et al.* (1978) were the first workers to report a laser flash method of measuring thermal diffusivity of liquid-saturated rocks. A laser was used to provide photothermal excitation of the front surface of a thin disc-shaped sample. The temperature rise was subsequently recorded intrusively at the rear surface by attached probes. The overall contacting nature of the foregoing methods has caused difficulties in the measurement of thermal diffusivity, which prompted Somerton (1992) to advocate 'that calculation of thermal diffusivity [rather than measurement] may be the better approach'.

In this paper for the first time we report as an initial/pilot study the application of laser-induced frequency-domain infrared photothermal radiometry (FD-PTR) to the measurement of thermal diffusivity of samples taken from limestone, calcarenite and marble statuary pedestals from Cyprus. The harmonic generation of thermal waves in these samples, and the totally non-contact character of FD-PTR coupled with the high noise rejection of lock-in analyser demodulation, have allowed high resolution measurements leading to meaningful correlations regarding the characterization of the samples' texture and possibly origins.

EXPERIMENTAL AND LITHOLOGY

Figure 1 shows the FD-PTR experimental set-up: a continuous wave (CW) Innova 100 Ar-ion laser from Coherent was used as an unfocused pump beam of spot size approximately 1.5 cm with output power of the order of 2.5 W at 514.5 nm. The intensity of the laser was harmonically modulated using an external square-waveform pulse generator to drive the acousto-optic modulator (AOM) and to change automatically the modulation frequency applied to it. The frequency scan was confined to the 0.16–4.0 Hz range, consistent with the thermal energy transport rates across the bulk of the sets of samples studied in this work.

The blackbody radiation from the photothermally excited stones was collected, mostly in the transmission configuration (not shown in Fig. 1), so as to yield the average value of the thermal diffusivity of the slices of stones, averaged over the entire thickness of the slice. The

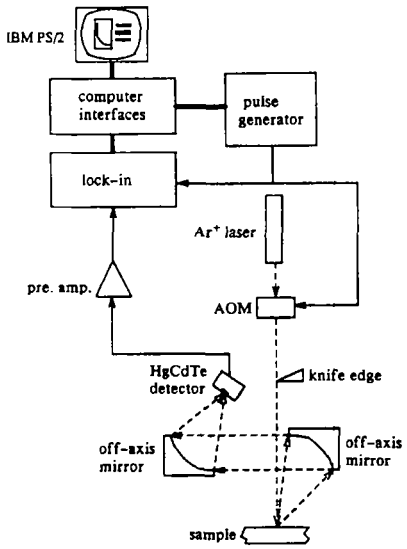

Figure 1 *Experimental set-up for back-scattered or transmission frequency-scanned PTR. AOM: acousto-optic modulator. HgCdTe detector: EG&G Judson Model J15-D12, dc-coupled with fitted Germanium window.*

alternative backscattered configuration shown in Figure 1 would be more appropriate for measurements with raw (unsliced) intact stones, conforming to the semi-infinite geometry. Two Ag-coated off-axis paraboloidal mirrors were used to capture and collimate the infrared radiation and, subsequently, to focus it on the active area of a Mercury-Cadmium-Telluride (MCT: HgCdTe) detector/preamplifier circuit with frequency bandwidth between dc and 1 MHz. The detector was fitted with a Ge window, which filtered out the excitation beam. The spectral response bandwidth of the detector was in the 8 to 12 μm range. The FD-PTR signal from the preamplifier (EG&G Judson model PA-350) was fed into the lock-in analyser (EG&G model 5210). This set-up allowed for computer-controlled, automatic frequency scans of the acousto-optically modulated laser intensity. The amplitudes and phases of the PTR signals were stored in an IBM PS/2 computer for theoretical analysis and calculations.

Thirteen pedestal stones collected from various locations on the island of Cyprus were studied. The samples were labelled according to their origin as shown on Table 1. Apart from sample PP2, an imported marble, the rest of the stones were limestones. These include several types of white through dark grey and light red dense fragmental limestones (samples PP1, PP3, PP4 and PP7 from Palaeopaphos) and from two quarries in the Paphos district from which similar stone is still being extracted (samples S1, S2 Souskiou, and PH1, PH2, PH3 Phasoula). Furthermore, a few cream-coloured calcarenites were included (samples PP5, PP6 Palaeopaphos and sample KQ3 from the Kouklia quarry). Intra-source homogeneity in samples from the various quarries was minimal with respect to crystallinity. All samples were overwhelmingly composed of carbonate (calcite) varying from microcrystalline to coarsely crystalline. They were mostly from rock types used for pedestals in Hellenistic and Roman times (Souskiou, Phasoula). Other types of samples are known to have been used for statues during those and earlier periods. The sample KQ3 from Kouklia may well be a non-artefact and therefore a calcarenite. Limestones among

Table 1 *Label identifiers of archaeological statuary pedestal stones tested, as per the location of their origin in Cyprus*

Stone label	*Origin (quarry)*
S1, S2	Souskiou[1]
PH1, PH2, PH3	Phasoula[2]
PP1, PP3, PP4, PP5, PP6, PP7	Palaeopaphos[3]
PP2	Palaeopaphos (import to Cyprus)[4]
KQ3	Kouklia[5]

[1] Petra tou Romiou limestone, light grey colour.
[2] Petra tou Romiou limestone, off-white colour.
[3] PP1: light pink, brecciated Petra tou Romiou limestone; PP3: grey, dense, pelagic limestone; PP4: dark grey crystalline limestone, possibly from the Kyrenia region; PP5 and PP6: light yellow medium-grained calcarenite; PP7: red, brecciated Petra tou Romiou limestone.
[4] PP2: coarsely crystalline light grey marble.
[5] KQ3: light yellow, medium-to-fine-grained calcarenite.

the samples could be differentiated either by visual or, in some instances, by hand lens examination. All of the limestones have been assigned to one of the oldest geological formations exposed in Cyprus with ages of roughly 200 Ma. The calcarenites are considerably more recent (*c.* 15 Ma).

For the present exploratory study it was deemed most appropriate to produce thin flat specimens of each stone under consideration. This type of sample geometry is most suitable for assessing quantitatively the sensitivity of PTR to small differences in thermal diffusivity by use of a simple one-dimensional (1-D) theoretical thermal-wave model in which the sample thickness is well defined and accurately measured independently (see 'PTR theory in archaeometry' below). The proposed sample preparation, of course, negates the otherwise inherently non-destructive character of the PTR technique. Once the sensitivity of PTR to limestone and marble stones is established in this work, in future applications, *in-situ* non-intrusive measurements of thermal diffusivity may be possible using a three-dimensional analogue: with tightly focused pump laser beam, the thermal-wave signal can be monitored at a radial position on a stone adjacent to the optically heated spot and the thermal diffusivity can be measured from the (known) radial distance and a modulation frequency scan, or from a fixed-frequency radial distance scan using a three-dimensional thermal-wave model (Mandelis forthcoming).

Based on the foregoing considerations, using a diamond-bladed metal saw, a piece from each stone was sliced into three flat slices of approximately 1.5 mm thickness and lateral dimensions large (typically $2 \times 1.5\,cm^2$) compared to the size of the incident laser beam. This geometry, coupled with the *c.* 1 cm-diameter laser beamwaist, is amenable to 1-D signal analysis of the PTR data (Rosencwaig and Gersho 1976). The accuracy of the thicknesses was ±2% of the measured thickness. PTR measurements on all three slices from each stone gave mean values and variances of the thermal diffusivity. Owing to the translucent nature of the Cypriot stones, the theoretical analysis of the data had to account for the finite optical absorption coefficient of the 514.5 nm radiation incident on the samples which tends to modify the heat deposition profile in the sample bulk. In many cases profuse scattering of the light at grain boundaries, veins and other types of defects

could be observed throughout the sample volume. For this reason, the optical absorption coefficients calculated from experimental data contained an unknown degree of contribution from scattering coefficients and could only be used as indicators to characterize each sample, rather than as absolute quantities. Therefore, they were defined as 'effective optical absorption coefficients'. An important advantage of PTR is that the blackbody signal is largely insensitive to scattered radiation, since it originates in the *thermally converted* optical energy; it does not depend on photon counts; and the incident and scattered radiation is efficiently blocked out of the detector element by narrowband infrared filters. Therefore, the thermal diffusivity values obtained in this work are considered absolute, albeit they were determined simultaneously with the 'effective' optical absorption coefficients. Excellent agreement with published values of thermal diffusivities of various rocks, in general (Touloukian and Ho 1981), and with limestones, in particular (Mongelli *et al.* 1982), further strengthens the foregoing argument on the absolute nature of our thermophysical measurements.

PTR THEORY IN ARCHAEOMETRY

It is well known that for small increases in the temperature, ΔT, of a solid due to a surface or bulk-distributed thermal source, the magnitude of the blackbody (Planck) radiation emitted by the solid when integrated over the entire emission spectrum is directly proportional to the temperature increment (Tam 1987; Tom *et al.* 1982):

$$S_B(\Delta T) = C\Delta T \tag{1}$$

where C is a constant which depends on the ambient temperature, T_o, and on the surface emissivity of the sample. Equation (1) is valid for small temperature excursions in the limit

$$\Delta T \ll T_o \tag{2}$$

Assuming a one-dimensional geometry corresponding to the stone samples used in this work (Fig. 2), three coupled heat diffusion equations can be written for harmonic optical heating of the samples at angular modulation frequency $\omega = 2\pi f$ (Carslaw and Jaeger 1959):

$$\frac{d^2\Delta T_g(x,\omega)}{dx^2} - \sigma_g^2 \Delta T_g(x,\omega) = 0, \quad x \leqslant 0 \quad \text{and} \quad x \geqslant L \tag{3}$$

$$\frac{d^2\Delta T_s(x,\omega)}{dx^2} - \sigma_s^2 \Delta T_s(x,\omega) = -\frac{I_o \eta \beta_s}{2k_s} e^{-\beta_s x}, \quad 0 \leqslant x \leqslant L \tag{4}$$

where I_o is the incident laser intensity, η is the optical-to-thermal energy conversion efficiency of the stone (assumed equal to unity), β_s is the sample optical absorption coefficient, k_s is the sample thermal conductivity, and σ_j is the complex thermal diffusion coefficient of medium $j[j = g$ (gas; air), s (solid)], defined as

$$\sigma_j = (1 + i)(\omega/2\alpha_j)^{1/2} \tag{5}$$

where α_j is the thermal diffusivity of material region (j).

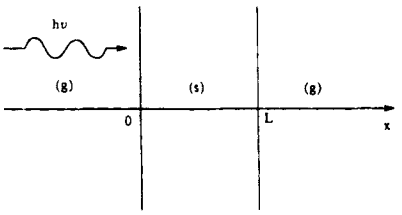

Figure 2 *Schematic of one-dimensional geometry for infrared photothermal radiometry of a slice of an archaeological stone;* (g): *gas (air) layer, and* (s): *solid layer of thickness* L, *thermal diffusivity* α_s *and effective optical absorption coefficient* β_s.

The solutions of the ordinary differential equations (3–4) are:

$$\Delta T_g(x \leqslant 0, \omega) = C_1 e^{\sigma_g x} \tag{6a}$$

$$\Delta T_s(x, \omega) = C_2 e^{-\sigma_s x} + C_3 e^{\sigma_s x} - \theta(x, \omega) \tag{6b}$$

$$\Delta T_g(x \geqslant L, \omega) = C_4 e^{-\sigma_s (x - L)} \tag{6c}$$

Here, $\theta(x, \omega)$ is given by

$$\theta(x, \omega) = \frac{I_o \eta \beta_s}{2k_s(\beta_s^2 - \sigma_s^2)} e^{-\beta_s x} \tag{7}$$

and $C_1, \ldots, C_4$ are integration constants which can be uniquely defined by boundary conditions of temperature and heat flux continuity at both interfaces $x = 0, L$:

$$\Delta T_s(x, \omega) = \Delta T_g(x, \omega) \quad \text{at} \quad x = 0 \quad \text{and} \quad L \tag{8a}$$

$$k_s \frac{d}{dx} \Delta T_s(x, \omega) = k_g \frac{d}{dx} \Delta T_g(x, \omega) \quad \text{at} \quad x = 0 \quad \text{and} \quad L. \tag{8b}$$

Calculating the integration constants from the four boundary conditions (8a, b), and inserting the expressions for C_2 and C_3 in Eq. (6b) yields for the value of the thermal-wave field at the rear surface ($x = L$) of the sample:

$$\Delta T_s(L, \omega) \simeq \frac{I_o \eta \beta_s}{2k_s \sigma_s^2 (r_s^2 - 1)} \left[\frac{2(r_s + b_{gs}) e^{-\sigma_s L}}{1 - e^{-2\sigma_s L}} - e^{-\beta_s L} - r_s \left(\frac{1 + e^{-2\sigma_s L}}{1 - e^{-2\sigma_s L}} \right) e^{-\beta_s L} \right] \tag{9}$$

The two new symbols r_s and b_{gs} are defined as follows:

$$r_s \equiv \beta_s / \sigma_s; b_{gs} = \frac{k_g \sqrt{\alpha_s}}{k_s \sqrt{\alpha_g}} \tag{10}$$

The approximate equality sign in Eq. (9) is there to indicate that the approximation $1 \pm b_{gs} \simeq 1$ was made. This approximation is very good for gas-solid systems, where $b_{gs} \sim 10^{-2} - 10^{-3}$ (Rosencwaig 1980).

For the special case of optically opaque solids, that is $\beta_s L \gg 1$, the expression for the rear-surface thermal-wave field, Eq. (9), simplifies to

$$\Delta T_s(L, \omega) = \frac{I_o \eta}{k_s \sigma_s} e^{-\sigma_s L} \tag{11}$$

Similarly, for the special case of thermally thick solids, that is $|\sigma_s| L \gg 1$, Eq. (9) becomes:

$$\Delta T_s(L,\omega) = \frac{I_o \eta r_s}{2k_s\sigma_s(1-r_s)} e^{-\beta_s L} \tag{12}$$

In the case of archaeological stones from Cyprus none of these simple limiting expressions was applicable. Therefore, the general formula, Eq. (9), had to be used in the PTR signal, Eq. (1) where C now incorporates an instrumental constant as well. It ought to be mentioned that Eq. (9) represents both the thermal-wave field at the rear surface of the solid *and* the blackbody radiation field, provided that the infrared absorption coefficient $\beta_s'(\lambda_{IR})$ in the emission wavelength, λ_{IR}, range of the sample is high enough for that emission to be fully re-absorbed by the solid (Leung and Tam 1984). This was assumed to be the case with the stones from Cyprus. If this assumption is not strictly valid, a contribution to the effective optical absorption coefficient β_s from $\beta_s'(\lambda_{IR})$ is expected, without any significant impact in the predicted value of thermal diffusivity.

In order to make the developed theoretical PTR model comply with the experimentally available lock-in analyser signal channels amplitude and phase, the complex Eq. (9) was transformed into an equivalent polar coordinate representation for direct use with the data:

PTR amplitude

$$|\Delta T_s(L,\omega)| = \frac{CI_o\eta}{2\sqrt{2}k_s a_s}\frac{|Z_4|}{|Z_5|}[(2Q_1\cos\psi_1 - e^{-\beta_s L}\cos\psi_2 - Q_2\cos\psi_3)^2 + (2Q_1\sin\psi_1 + e^{-\beta_s L}\sin\psi_2 - Q_2\sin\psi_3)^2]^{1/2} \tag{13}$$

PTR phase

$$\phi(L,\omega) = \tan^{-1}\left[\frac{2Q_1\sin\psi_1 + e^{-\beta_s L}\sin\psi_2 - Q_2\sin\psi_3}{2Q_1\cos\psi_1 - e^{-\beta_s L}\cos\psi_2 - Q_2\cos\psi_3}\right] \tag{14}$$

where the various quantities have been defined in the Appendix.

PTR RESULTS, PETROGRAPHY AND CORRELATIONS

PTR frequency responses

A few preliminary attempts were made to modify the stone surfaces to simplify the quantitiative analysis by depositing a thin black layer on the surface, which would render the samples opaque and would validate Eq. (11). Ink and soot layers were deposited, but both approaches were abandoned. The former resulted in irreversible penetration of ink in some stones through grain boundaries or other macroscopic defect structures, including pores. The ink coating could not be removed through vigorous washing and there was concern that seepage could modify the heat conduction path-ways, thus producing erroneous thermal diffusivity values. Furthermore, it appeared that the application of a thin soot layer from a candle flame may have caused some permanent thermal change in the stone structure, as witnessed by irreversible changes in the calculated values of α_s before and after the application of the candle flame. Therefore, the results shown below were obtained without any stone surface preparation and yielded very reproducible values of the diffusivity. In Figures 3–5 the experimental radiometric data

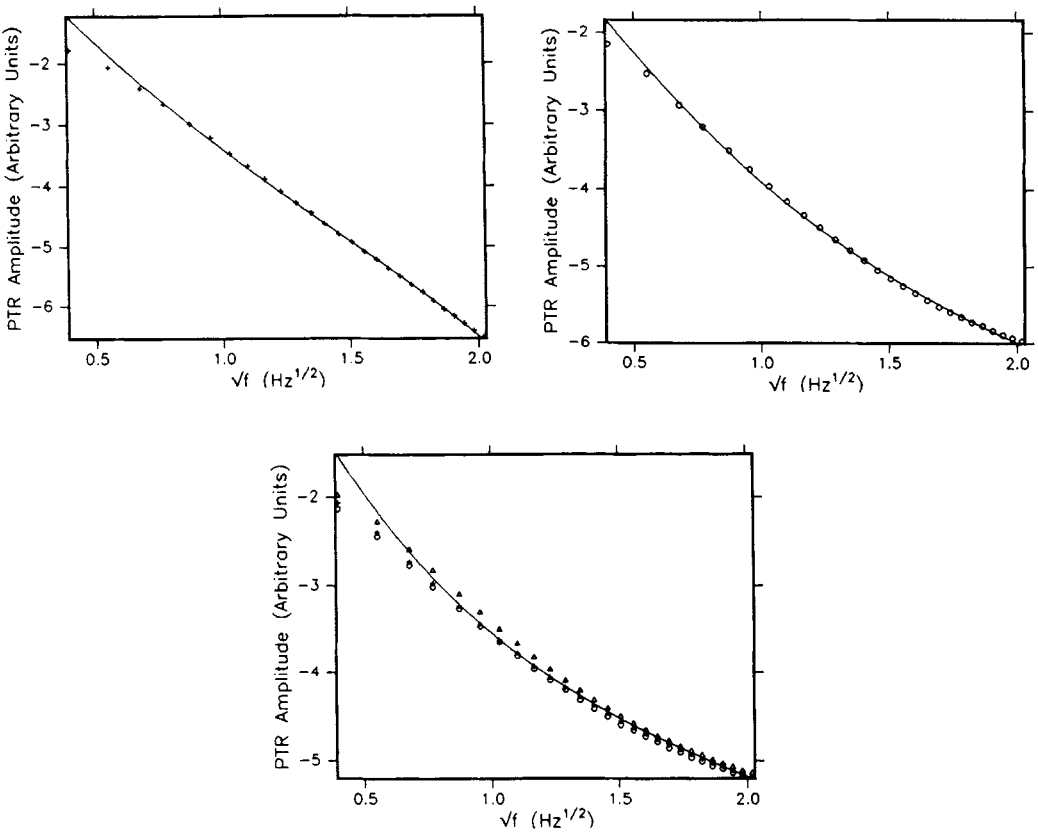

Figure 3 *PTR amplitude versus* $f^{1/2}$ *data.* (Upper left): *data from the stone PP7. Best fit to the data was obtained with* $\alpha_s = 1.55 \times 10^{-6}\, m^2/s$ *and* $\beta_s = 39.7\, cm^{-1}$. (Upper right): *data from the stone PH2. Best fit to the data was obtained with* $\alpha_s = 1.57 \times 10^{-6}\, m^2/s$ *and* $\beta_s = 13.8\, cm^{-1}$. (Lower centre): *data from the anomalous stone PP2. The three experimental curves (discontinuous data points) are shown along with the best theoretical fit.*

were plotted versus the square root of frequency, as the most appropriate power of this control parameter, owing to the diffusive nature of the signal generation mechanism, that is the thermal wave in the rock: diffusive phenomena in simple homogeneous media in one spatial dimension evolve with the square root of time (Carslaw and Jaeger 1959), or, conversely, with the inverse square root of frequency. This can be seen in the simplified form of Eqs. (11) and (12) as $\Delta T_s \propto \sigma_s^{-1} \propto \omega^{-1/2}$.

Figure 3 (upper left) shows experimental frequency response data from a slice of stone PP7 and the theoretical fit to the amplitude data of Eq. (13). Only amplitude data fits were considered in this work. Phase frequency scans produce similar results. Three sets of data were obtained using three slices per stone. The curve-fitting involved the optimum adjustment of the α_s and β_s values. The excellent fit of the theory to the data in Figure 3 (upper left) is typical of all three PP7 slices, including the substantial deviation at $f < 0.2$ Hz. The origins of the deviation are associated with the non-flat instrumental frequency response (transfer function) at frequencies below 1 Hz, and they do not affect the relative values of the measured thermal diffusivities. It should be realized that the developed theoretical model assumes a totally homogeneous solid. The uniqueness of the two-parameter fit (α_s, β_s) to the data is

very good, because the high-frequency (thermally-thick (Rosencwaig and Gersho 1976), $f > 2$ Hz) regime of the plot in Figure 3 (upper left) is mostly sensitive to the value of β_s, whereas the low-frequency (thermally-thin (Rosencwaig and Gersho 1976), $f < 2$ Hz) regime is only sensitive to the value of α_s. Similar quality of agreement between theory and experiment was obtained with stones PP1 and PP3–PP6. In all these cases the discrepancy at the low-frequency end of the curves persisted, whereas decreased values of the effective β_s were found to be responsible for the change in the sign of the curvature at high frequencies in the PH series, Figure 3 (upper right). The shape of this frequency-response curve and the quality of the fit is typical of all three stones PH1–PH3. The same excellent fit was further obtained for stones KQ3, S1 and S2.

No satisfactory fit could be obtained from stone PP2 for any combination of parameter pairs (α_s, β_s). Figure 3 (lower centre) shows the three experimental curves from the three PP2 slices and the closest possible theoretical curve. The problem was that, in order to generate the steep upward curvature of the data lines, β_s had to be less than $10\,cm^{-1}$, which made the entire theoretical curve insensitive to thermal diffusivity, as back-surface heating was dominated by local optical absorption rather than bulk heat conduction. Therefore, no value of α_s was assigned to stone PP2. The use of a simple linear regression fit to the data, however, gave a thermal diffusivity value which was *c.* 15% higher than stone PP4 (when the data from the latter were treated with a similar linear regression method). It is believed that the anomalous stone PP2 failed to conform with the assumption of a single, homogeneous layer on which the theory was based, throughout the entire frequency range under investigation. Petrographic investigation (see below, 'Petrography') seemed to confirm this interpretation based on observations of lamellar twinning of bulk domains throughout this stone.

Table 2 shows the thermal diffusivity values and their variances obtained for all the stones, and Figure 4 represents groupings of these values based in stone types. Table 3 shows the

Table 2 *Mean values and variances of Cypriot archaeological stone thermal diffusivities (see Table 1). Results of three test samples per stone. The limit of the resolution of diffusivity values of the present PTR technique was found from this table to be* $\pm 0.05 \times 10^{-6}\ m^2/s$. *The numbers in parentheses indicate groupings of stones as per petrographic structure determination (see 'Petrography' and 'Discussion and conclusions')*

Stone label	*Mean thermal diffusivity* (m^2/s)	*Variance* $\pm\sqrt{((\Sigma\Delta\alpha^2)/3)}$ (m^2/s)
KQ3 (3)	0.93×10^{-6}	$\pm 0.10 \times 10^{-6}$
S1 (1)	1.55×10^{-6}	$\pm 0.19 \times 10^{-6}$
S2 (2)	1.28×10^{-6}	$\pm 0.04 \times 10^{-6}$
PH1 (1)	1.22×10^{-6}	$\pm 0.04 \times 10^{-6}$
PH2 (1)	1.57×10^{-6}	$\pm 0.10 \times 10^{-6}$
PH3 (1)	1.33×10^{-6}	$\pm 0.16 \times 10^{-6}$
PP1 (1)	1.43×10^{-6}	$\pm 0.07 \times 10^{-6}$
PP2 (4)	Undefined (>PP4)	
PP3 (2)	1.27×10^{-6}	$\pm 0.11 \times 10^{-6}$
PP4 (1)	1.70×10^{-6}	$\pm 0.09 \times 10^{-6}$
PP5 (3)	1.00×10^{-6}	$\pm 0.00 \times 10^{-6}$
PP6 (3)	0.87×10^{-6}	$\pm 0.04 \times 10^{-6}$
PP7 (1)	1.55×10^{-6}	$\pm 0.00 \times 10^{-6}$

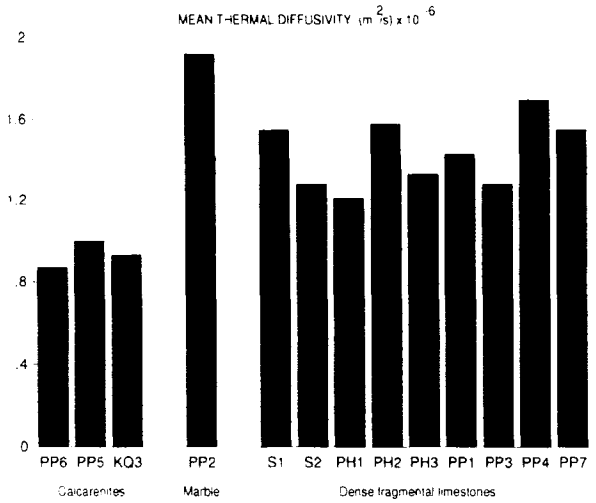

Figure 4 *Thermal diffusivity grouping histograms showing clear value range separation among calcarenites, dense fragmental limestones and marble.*

respective effective optical absorption coefficient values. It will be noticed that the spread in β_s variances is much larger than that in α_s variances. This is the result of optical scattering in the various test specimens and its strong dependence on variations in defect/grain/crystallite structures from sample to sample. The range of measured thermal diffusivities in Table 2, $0.9–1.7 \times 10^{-6}$ m^2/s is in excellent agreement with values for limestone reported at room temperature by Mongelli *et al.* (1982). They also exhibit agreement within a factor of two with values reported for other rocks, for example, quartzite, dolomite and mica-quartzite (Mongelli *et al.* 1982); granite, basalt and sandstone (Hanley *et al.* 1978; Touloukian and Ho 1981); diorite, diabase, feldspars and garnets (Touloukian and Ho 1981).

Table 3 *Mean values and variances of Cypriot archaeological stone effective optical absorption coefficients corresponding to entries in Table 2*

Stone label	*Mean effective absorption coefficient* cm^{-1}	*Variance* $\pm\sqrt{((\Sigma\Delta\beta^2)/3)}$ (cm^{-1})
KQ3	48.7	±5.0
S1	18.0	±4.3
S2	27.2	±5.2
PH1	19.7	±2.6
PH2	13.8	±1.0
PH3	13.2	±0.5
PP1	38.5	±4.1
PP2	< 8.0	
PP3	39.7	±3.7
PP4	18.8	±4.9
PP5	35.0	±2.4
PP6	46.0	±1.1
PP7	39.7	±0.9

Petrography

Following the PTR study, a thin slice was cut from each stone and these thin samples were prepared for examination with the petrographic microscope of the Department of Earth Sciences, University College, London, U.K. The results of the petrographic analysis were as follows.

(a) Stones S1 and S2 from the Souskiou quarry were cream- and grey-coloured, respectively, in agreement with the trend in β_s shown in Table 3. They were dense, fine-grained limestones and consisted of rounded to sub-rounded areas of microgranular calcite and rare bivalve shell fragments surrounded by fine- to coarse-grained crystalline calcite. Veins through the stones were invariably filled with coarsely crystalline calcite. Most importantly, the two stones also differed in the degree of crystallinity, with S1 being decidedly more crystalline (approx. 40% microgranular calcite) than S2 (approx. 70% microgranular calcite). These differences are in agreement with the higher diffusivity of S1, as expected from more highly atomically ordered (i.e. more crystalline) solids.

(b) The three samples from the Phasoula quarry (PH1, PH2, PH3) were white- to cream-coloured dense fragmental limestones considered to be of similar age and to belong to the same geological formation as those from the Souskiou quarry (S1 and S2). The similar β_s values among S1, PH1, PH2 and PH3 are in agreement with the exhibited colours. Microscopic examination showed that they consisted of microgranular calcite (approx. 70% by volume in PH3 and 50% in PH1, PH2). The remainder was fine- to coarse-grained holocrystalline calcite. From Table 2 it can be seen that the petrographic analysis is consistent with the diffusivities of PH3 (similar to S2) and the more crystalline PH2 (similar to S1); the diffusivity of PH1 is closer to PH3 than to PH2 and thus appears somewhat anomalous. Nevertheless, the range of diffusivity values of the Phasoula quarry group is identical to those of the Souskiou quarry stones, very likely a manifestation of their common geological origins.

(c) The Palaeopaphos samples PP1, PP4 and PP7 were dense fragmental limestones. Those stones were pink, grey to dark grey and red in colour, respectively. No clear pattern in effective optical absorption coefficients emerges from Table 3. PP1 and PP7 mainly consisted of microgranular calcite (approx. 80% PP1 and 70% PP7) carrying very small spheroidal masses of fine-grained crystalline calcite. Veins were abundant and made up the remainder of each sample; they consisted of medium- to coarse-grained crystalline calcite. The very similar thermal diffusivities of PP1 and PP7 are consistent with the very similar texture of these stones. Sample PP4 differed in that it exhibited almost total absence of microgranular calcite; its place had been taken by fine crystalline calcite, resulting in higher thermal diffusivity than samples PP1 and PP7, as expected.

In contrast to the above, stone PP2 was a greyish-white, medium- to coarse-grained marble, an unprovenanced import to the island of Cyprus, consisting almost entirely of anhedral (granular) holocrystalline calcite with ubiquitous lamellar twinning and scarce magnetite grains. The dominantly crystalline nature of that stone was consistent with our approximate (linear regression) calculations of its thermal diffusivity, which indicated values higher than the highest of the group, sample PP4. The lamellar structure of stone PP2 was most likely the cause of its failure to comply with the single continuous layer description built in to the theoretical photothermal model above ('PTR theory in archaeometry').

Stones PP5 and PP6 represented an entirely different type of rock which, nevertheless, essentially consisted of calcium carbonate. In both stones, *c.* 95% of the bulk by volume was made of micritized foraminiferal tests and of bivalve and algal fragments in a matrix of microgranular calcite with some fine-grained crystalline calcite. The remainder of the stone bulk was made of non-carbonate clasts (*c.* 5% by volume). Those were represented by broken crystals of quartz, feldspar and chlorite. Although it is hard to make detailed predictions of the values of thermal diffusivity expected from stones PP5 and PP6, it is clear from Table 2 that the calculated values are considerably lower than those of the PP1, PP4, PP7 group, perhaps owing to the abundant grain boundary/fragmental structure of the PP5, PP6 stones which would impede transient heat flow across the bulk of these samples.

(d) The stone KQ3 was collected from an old quarry near the village of Kouklia. Petrographically it was found to be identical to stones PP5 and PP6 and might have been the source for the Palaeopaphos samples in antiquity. It is important to note that its thermal diffusivity was also found to be identical (within statistical variance) with those of the PP5, PP6 pair.

(e) The stone PP3, a grey dense pelagic limestone, consisted of *c.* 60% microgranular calcite. The remainder was small spheroidal masses (original radiolaria?) of fine-grained crystalline calcite. Thin veins were filled with finely crystalline calcite. The similarity in its thermal diffusivity value to those of the similarly structured PP1, PP7 pair (within statistical variance) is also consistent with the foregoing description.

DISCUSSION AND CONCLUSIONS

In this work infrared radiometry was adapted and applied to the investigation of archaeological stones from Cyprus in a feasibility study aiming to introduce experimentally and theoretically a novel non-contact, potentially non-intrusive technique of laser photothermal archaeometry of high enough sensitivity to resolve small differences in the thermal diffusivity of ancient samples. Although the limited set of samples examined was of insufficient quantity to perform detailed studies on source homogeneity variations, visual examination in the quarries indicated adequate source homogeneity, so as to allow the present study to obtain particular thermal diffusivity ranges from specific quarries. The purpose of the current investigation was to determine whether thermal diffusivity could be used as a finger-printing diagnostic method for the characterization of rock materials. Carbonate rocks were selected, since most ancient statuary traded around the known world in Hellenistic and Roman times and earlier periods was manufactured from these rock types. These carbonate rocks fell into four petrographic broad groups: (1) dense fragmental limestones (S1, S2, PH1, PH2, PH3, PP1, PP4 and PP7); (2) dense fine-grained pelagic limestone (PP3); (3) calcarenites (PP5, PP6 and KQ3); and (4) crystalline marble (PP2) which could easily be differentiated by anyone with some geological expertise.

Although the stones from Cyprus exhibited rather complex structure, the excellent agreements between PTR frequency response curves and theoretical curve-fits for all the samples, with one exception (PP2), strongly supported the thermal behaviour of these stones as virtually homogeneous, continuous solid layers, along the fundamental assumption of the developed one-dimensional PTR theory. Therefore, the thermal diffusivity values compiled in Table 2 can be taken as true representations of the thickness-averaged mean value for each sample. Table 2 and Figure 4 showed relatively clear divisions of the

three groups (the limestone groups (1) and (2) were merged) in terms of diffusivity values. No clear trends could be established in terms of effective optical absorption coefficients, Table 3. This is not surprising, since the light scattering properties of the various stones were widely different and slice dependent, which tended to yield erroneous values for the true optical absorption coefficients. On the contrary, photothermal detection is known to be less sensitive or insensitive to light scattering processes, because it does not depend on photon counting (Per Helander 1983).

From Table 2 the following groupings can be observed: (1) dense fragmental limestones ($\alpha_s = 1.22 - 1.70 \times 10^{-6}\,m^2/s$), including dense fine-grained pelagic limestones ($\alpha_s = 1.27 \times 10^{-6}\,m^2/s$); (2) calcarenites ($\alpha_s = 0.87 - 1.00 \times 10^{-6}\,m^2/s$); (3) marbles ($\alpha_s \sim 15\%$ higher than $1.70 \times 10^{-6}\,m^2/s$).

The above considerations show that thermal diffusivity could be used as an aid to discrimination in sourcing studies of archaeological stone artefacts. If colour is not taken into account, then pedestals PP1, PP4 and PP7 could have originated in either the Souskiou or the Phasoula quarries. Since the particular coloration of these pedestals is absent from those quarries, the foregoing pedestals are commonly not thought to come from the Souskiou or the Phasoula quarries. In terms of thermal diffusivity diagnostics, it is clear that stone crystallinity content determines thermal diffusivity, with the higher crystalline content stones exhibiting higher diffusivity. The preliminary success of laser PTR archaeometry reported in this work as a high-resolution thermal-diffusivity intrumentation and measurement methodology will be further tested by using holocrystalline materials (marbles). This further work is under preparation and should determine whether small compositional variants can be resolved via the measurement of thermal diffusivity values.

ACKNOWLEDGEMENTS

The authors are thankful to Dr M. Munidasa for helping out with PTR instrumentation adjustments and modifications to accommodate the novel laser photothermal archaeometric configuration. A McAllister Summer Student Award to one of us (K.M.A.) is gratefully acknowledged. Thanks are also extended to Professor Alaim Load of the Department of Earth Sciences, University College London, U.K., for the preparation of thin samples.

REFERENCES

Boozer, G. D., 1958, *A method of measuring the thermal diffusivity of consolidated materials at elevated temperatures*, unpubl. M.S. thesis, University of California, Berkeley.

Carslaw, H. S., and Jaeger, J. C., 1959, *Conduction of heat in solids*, 2 edn., Oxford University Press, London.

Gomaa, E., 1973, *Thermal behavior of partially liquid saturated porous media*, unpubl. Ph.D. dissertation, University of California, Berkeley.

Hanley, E., DeWitt, D., and Roy, R., 1978, Thermal diffusivity of eight well-characterized rocks of temperature range 300-1000 °K, *Engin. Geol.*, **12**, 31–47.

Hirsch, J., 1973, *Transient method for measuring thermal properties of rocks*, M.S. Res. Rep., University of California, Berkeley.

Leung, W. P., and Tam, A. C., 1984, Techniques of flash radiometry, *J. Appl. Phys.*, **56**, 153–61.

Mandelis, A., forthcoming, Green's functions in thermal wave physics: Cartesian coordinate representations, *J. Appl. Phys.*

Mongelli, F., Loddo, M., and Tramacue, A., 1982, Thermal conductivity, diffusivity, and specific heat variation of some Travale Field (Tuscany) rocks versus temperature, *Tectonophysics*, **83**, 33–43.

Mossahebi, M., 1966, *Thermal conductivity of rocks by a ring source device*, unpubl. M.S. thesis, University of California, Berkeley.

Nguyen, T., 1974, *Transient method of measuring thermal properties of rocks at elevated pressures and temperatures*, M.S. Res. Rep., University of California, Berkeley.

Per Helander, O.F., 1983, *Optical spectroscopy using an open photoacoustic cell*, unpubl. Ph.D. dissertation, Linköping, Sweden.

Rosencwaig, A., 1980, *Photoacoustics and photoacoustic spectroscopy*, J. Wiley and Sons, New York.

Rosencwaig, A., and Gersho, A., 1976, Theory of the photoacoustic effect with solids, *J. Appl. Phys.*, **47**, 64–9.

Somerton, W. H., 1992, *Thermal properties and temperature-related behavior of rock/fluid systems*, Developments in Petroleum Science (ed. G. V. Chilingarian), **37**, Elsevier, Amsterdam.

Somerton, W. H., and Boozer, G. D., 1960, Thermal characteristics of porous rocks at elevated temperatures, *J. Petrol. Technol.*, **12**, 77–81.

Somerton, W. H., and Boozer, G. D., 1961, Method of measuring thermal diffusivities of rocks at elevated temperatures, *A.I.Ch.E.*, **7**, 87–90.

Tam, A. C., 1987, Pulsed laser photoacoustic and photothermal detection, in *Photoacoustic and thermal wave phenomena in semiconductors* (ed. A. Mandelis), 175–200, North-Holland, New York.

Tom, R. D., O'Hara, E. P., and Benin, D., 1982, A generalized model of photothermal radiometry, *J. Appl. Phys.*, **53**, 5392–400.

Touloukian, Y. S., and Ho, C. Y., 1981, *Physical properties of rocks and minerals*, McGraw-Hill, New York.

APPENDIX: DEFINITIONS OF CONSTANTS APPEARING IN EQS. (13–14)

$$a_s \equiv (\omega/2\alpha_s)^{1/2} \tag{A.1}$$

$$|Z_1| = \left[\left(\frac{\beta_s}{2a_s} + b_{gs}\right)^2 + \left(\frac{\beta_s}{2a_s}\right)^2\right]^{1/2} \tag{A.2}$$

$$\phi_1 = -\tan^{-1}\left[\frac{(\beta_s/2a_s)}{(\beta_s/2a_s) + b_{gs}}\right] \tag{A.3}$$

$$|Z_2| = [(1 - e^{-2a_s L}\cos 2a_s L)^2 + e^{-4a_s L}\sin^2 2a_s L]^{1/2} \tag{A.4}$$

$$\phi_2 = \tan^{-1}\left(\frac{e^{-2a_s L}\sin 2a_s L}{1 - e^{-2a_s L}\cos 2a_s L}\right) \tag{A.5}$$

$$|Z_3| = [(1 + e^{-2a_s L}\cos 2a_s L)^2 + e^{-4a_s L}\sin^2 2a_s L]^{1/2} \tag{A.6}$$

$$\phi_3 = -\tan^{-1}\left(\frac{e^{-2a_s L}\sin 2a_s L}{1 + e^{-2a_s L}\cos 2a_s L}\right) \tag{A.7}$$

$$|Z_4| = \beta_s/\sqrt{2}a_s \tag{A.8}$$

$$\phi_4 = \frac{\pi}{4} \tag{A.9}$$

$$|Z_5| = [(\beta_s^4/4a_s^4) + 1]^{1/2} \tag{A.10}$$

$$\phi_5 = \pi + \tan^{-1}(\beta_s^2/2a_s^2) \tag{A.11}$$

$$Q_1 \equiv \frac{|Z_1|}{|Z_2|}e^{-a_s L} \tag{A.12}$$

$$Q_2 \equiv \frac{|Z_3||Z_4|}{|Z_2|}e^{-\beta_s L} \tag{A.13}$$

$$\psi_1 \equiv \phi_1 - \phi_2 - \phi_5 - a_s L - \frac{\pi}{2} \tag{A.14}$$

$$\psi_2 \equiv \phi_5 + \frac{\pi}{2} \tag{A.15}$$

$$\psi_3 \equiv \phi_3 - \phi_2 - \psi_2 + \phi_4 \tag{A.16}$$